

Simulation Analysis of Balance Detection Technique in Coherent Optical Receiver

Piaokun Zhang, Zhongwei Tan*, Zhichao Ding, Lijun Guo

Key Laboratory of All Optical Network & Advanced Telecommunication Network of EMC, Institute of Lightwave Technology, Beijing Jiaotong University, Beijing, China

Email: 19125071@bjtu.edu.cn, *zhwtan@bjtu.edu.cn, 17111006@bjtu.edu.cn, 19120052@bjtu.edu.cn

How to cite this paper: Zhang, P.K., Tan, Z.W., Ding, Z.C. and Guo, L.J. (2021) Simulation Analysis of Balance Detection Technique in Coherent Optical Receiver. *Optics and Photonics Journal*, 11, 301-313. <https://doi.org/10.4236/opj.2021.118020>

Received: March 23, 2021

Accepted: July 31, 2021

Published: August 3, 2021

Abstract

This paper introduces the working principle of the balanced heterodyne detection system, establishes the corresponding mathematical model, deduces the signal to noise ratio (SNR) formula of the balanced heterodyne detection. By comparing balance heterodyne detection with general coherent detection with MATLAB numerical simulation, the superiority of balance heterodyne detection system is proved theoretically. Finally, the simulation models of ordinary heterodyne detection, balance detection and double balance detection system are built by OptiSystem. The simulation results are consistent with the conclusions derived from the mathematical analysis, which provides a new method for the research of weak laser detection technology.

Keywords

Balance Heterodyne Detection, 90° Optical Mixer, Signal to Noise Ratio, The Numerical Simulation

1. Introduction

As early as the 1980s, optical coherence detection technology has been focusing in the field of optical communication [1]. The balance detection and double balance detection system were proposed during this period [2]. In 1985, Gregory *et al.* proposed the concept of balanced detection, that two photoelectric detectors with nearly identical parameters were simultaneously used in a photoelectric detection unit, and the signal light and local oscillator light were incident into the two photoelectric detectors respectively. Then the high-frequency signals were filtered through the difference circuit to obtain the required medium-frequency signals [3]. The balance heterodyne detection overcomes the disadvantage of low utilization rate of local oscillator in single tube detection,

which allows that the coherent optical communication receiver obtains high sensitivity and SNR at lower local oscillator power. The balance heterodyne detection can also effectively suppress the interference of common mode noise and improve the SNR of coherent optical communication system close to the quantum noise limit level [4]. The double balance detection technology was developed by Kuwaharra *et al.* on the basis of the balance detection theory in 1987. It not only has the advantages of the balance detection technology, but also has a variety of modulation and demodulation methods, as well as good environmental adaptability and better system stability [5].

In this paper, through the derivation of the mathematical model of balance detection, MATLAB is used to analyze the SNR of the balance detection and ordinary heterodyne detection. In addition, optical simulation software OptiSystem is used to build the simulation models of ordinary heterodyne detection, balance detection and double balance detection system.

2. Theoretical Derivation

2.1. Mathematical Model of Balance Detection Technique

As we all know, for IM/DD system directly incident light field on the photodetector only signal light $E_s(t)$, so the output of the detector should be:

$$S_{PD} = i_{PD}^2 R_L = \beta^2 P_S^2 R_L. \tag{1}$$

In Equation (1), β is the responsiveness of the photodetector.

Suppose the signal light of heterodyne detection is $E_s(t) = A_s \cos(\omega_s(t) + \phi_s)$, The local oscillator light is $E_L(t) = A_L \cos(\omega_L(t) + \phi_L)$, Then the output of ordinary heterodyne detection is [6]:

$$i_{PD} = \beta \overline{[E_s(t) + E_L(t)]^2} = \beta \left\{ \overline{A_s^2 \cos^2(\omega_s t + \phi_s)} + \overline{A_L^2 \cos^2(\omega_L t + \phi_L)} + A_s A_L \overline{\cos[(\omega_s + \omega_L)t + (\phi_s + \phi_L)]} + A_s A_L \overline{\cos[(\omega_s - \omega_L)t + (\phi_s - \phi_L)]} \right\}. \tag{2}$$

Due to the limitation of intermediate frequency bandwidth, the photodetector can only respond to the difference frequency term, then the final detected current signal is [7]:

$$i_{out} = \beta A_s A_L \cos[(\omega_s - \omega_L)t + (\phi_s - \phi_L)]. \tag{3}$$

The principle of balance detection is shown in **Figure 1**. After the signal light E_s and the local oscillator light E_L are input to the beam splitter B through the optical fiber, two signals lights (E_{s1} and E_{s2}) and two local oscillator lights (E_{L1} and E_{L2}) are generated respectively. Where E_{s1} and E_{L1} are received by photodetector 1 and output photocurrent $i1$; E_{s2} and E_{L2} are received by photodetector 2 and the output current is $i2$. The phase of the photocurrent output by the two detectors is opposite, and the final IF signal is obtained after the difference frequency.

It is known that the signal light of heterodyne detection is $E_s(t) = E_s \cos(\omega_s(t) + \phi_s)$, and the local oscillator light is

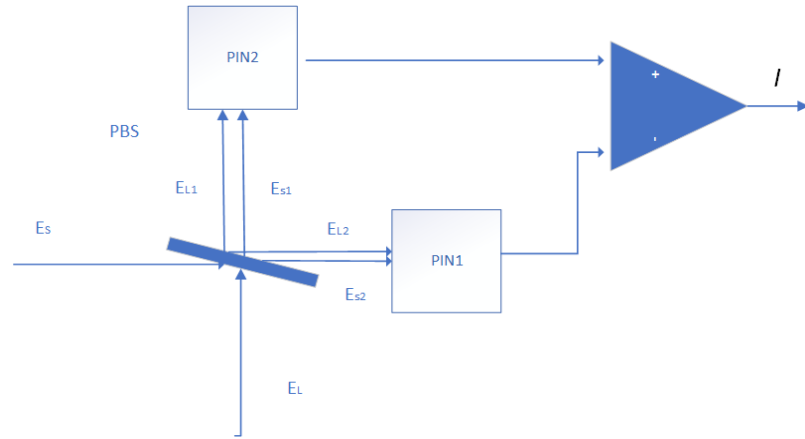


Figure 1. Schematic diagram of balance detection.

$$E_L(t) = E_L \cos(\omega_L(t) + \phi_L)$$

where: E_s, ω_s, ϕ_s and E_L, ω_L, ϕ_L are the amplitude, frequency and phase of the signal light and the local oscillator light respectively. Assuming that the fraction ratio of the beam splitter is ε , the quantum efficiency of the two detectors is η_1 and η_2 , and the bandwidth Δf is equal, the energy of the signal light and the local oscillator light after passing through the beam splitter can be calculated as [8] [9]:

$$\begin{aligned} E_{s_1} &= \sqrt{1-\varepsilon} E_s \cos(\omega_s(t) + \phi_s) \\ E_{s_2} &= \sqrt{\varepsilon} E_s \cos(\omega_s(t) + \phi_s) \\ E_{L_2} &= \sqrt{1-\varepsilon} E_L \cos(\omega_L(t) + \phi_L) \\ E_{L_1} &= \sqrt{\varepsilon} E_L \cos(\omega_L(t) + \phi_L) \end{aligned} \tag{3}$$

The output of the four-way signal after mixing with the photodetector is:

$$\begin{aligned} i_1 &= \frac{\eta_1 e}{h\omega} \left\{ (1-\varepsilon) E_s^2 + \varepsilon E_L^2 - 2\sqrt{1-\varepsilon}\sqrt{\varepsilon} \right. \\ &\quad \left. \times E_s E_L \cos[(\omega_s - \omega_L)t + \phi_s - \phi_L] \right\} + n_1 \\ i_2 &= \frac{\eta_2 e}{h\omega} \left\{ \varepsilon E_s^2 + (1-\varepsilon) E_L^2 + 2\sqrt{1-\varepsilon}\sqrt{\varepsilon} \right. \\ &\quad \left. \times E_s E_L \cos[(\omega_s - \omega_L)t + \phi_s - \phi_L] \right\} + n_2 \end{aligned} \tag{4}$$

In the Equation (4), $n_1(t)$ and $n_2(t)$ are noise currents. The response current signal of the final balanced detection system is as follows:

$$\begin{aligned} i &= i_2 - i_1 = \frac{e}{h\omega} \left\{ [\varepsilon\eta_2 - (1-\varepsilon)\eta_1] E_s^2 + [(1-\varepsilon)\eta_2 - \varepsilon\eta_1] E_L^2 \right\} \\ &\quad + \frac{e}{h\omega} \left\{ 2(\eta_1 + \eta_2) \sqrt{1-\varepsilon}\sqrt{\varepsilon} E_s E_L \times \sin[(\omega_s - \omega_L)t + \phi_s - \phi_L] \right\} \\ &\quad + \{n_2(t) - n_1(t)\}. \end{aligned} \tag{5}$$

The double balance detection system is based on the structure of the balance heterodyne detection system, which uses four almost identical photoelectric de-

tectors to form two groups of balance heterodyne detectors at the receiving end [10] [11] [12]. The photocurrent signal received by the detector is processed by differential processing to obtain the difference frequency signal. Its principle block diagram is shown in **Figure 2**.

The following mathematical model is used to illustrate this process.

Let the mathematical expression of the local oscillator light and the signal light be as follows:

$$E_L = \begin{bmatrix} k_1 \\ k_2 \end{bmatrix} \exp(i\phi)$$

$$E_S = \begin{bmatrix} k_3 \\ k_4 \end{bmatrix} \exp(i\omega_j t)$$
(6)

where, k_1, k_2, k_3 and k_4 represent the respective components of the local oscillator light and the signal light in two directions respectively.

Let E'_L be the circularly polarized light formed after the local oscillator light passes through the 1/4 wave plate, then:

$$E'_L = \begin{bmatrix} k_1 \exp(i\pi/2) \\ k_2 \end{bmatrix} \exp[i(\phi - \pi/4)].$$
(7)

After the two beams of light pass through the beam splitting prism, they are divided into two beams of light in the horizontal and vertical directions, and the beam splitting prism transmits and reflects the matrix.

$$T = \begin{bmatrix} t_{\parallel} \exp(i\tau_{\parallel}) & 0 \\ 0 & 0 \end{bmatrix}, R = \begin{bmatrix} 0 & 0 \\ 0 & r_{\perp} \exp(i\rho_{\perp}) \end{bmatrix}.$$
(8)

It can be obtained from the above equation.

$$E_1 = \begin{bmatrix} t_{\parallel} \exp(i\tau_{\parallel}) k_1 \exp[i(\phi + \pi/4)] \\ r_{\perp} \exp(i\rho_{\perp}) k_4 \exp(i\omega_j t) \end{bmatrix}$$

$$E_2 = \begin{bmatrix} t_{\parallel} \exp(i\tau_{\parallel}) k_3 \exp(i\omega_j t) \\ r_{\perp} \exp(i\rho_{\perp}) k_2 \exp[i(\phi + \pi/4)] \end{bmatrix}$$
(9)

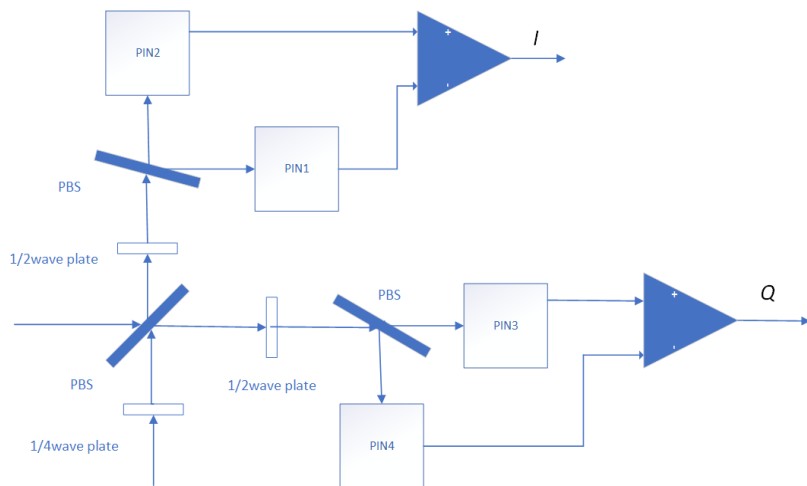


Figure 2. Schematic diagram of double balance detection.

The transmission matrix of 1/2 wave plate in the system is

$$\Lambda_{1/2} = \frac{\sqrt{2}}{2} \begin{bmatrix} 1 & 1 \\ 1 & -1 \end{bmatrix}. \quad (10)$$

In Equation (10), the angle between the wave plate and the X-axis is 22.5° .

Two beams of light through the beam splitter are divided into four different directions of the light signals, the photodetector after detection of the four channels phase difference $\pi/2$ photocurrent signal.

$$I_0 = \frac{1}{2} \left\{ k_1^2 + k_4^2 + 2k_1k_4 \cos \left[\omega_f t + \rho_\perp - \tau_\parallel - (\phi + \pi/4) \right] \right\}. \quad (11)$$

Similarly, the expressions of I90, I180 and I270 can be derived, which will not be expanded in detail here. Four channels of signal for differential processing, obtained two groups of phase difference $\pi/2$ differential signals, namely orthogonal component I and vertical component Q .

$$\begin{aligned} I : I_0 - I_{180} &= 2k_1k_4 \cos \left[\omega_f - (\phi + \pi/4) \right] \\ Q : I_{90} - I_{270} &= 2k_2k_3 \sin \left[\omega_f - (\phi + \pi/4) \right] \end{aligned} \quad (12)$$

Compared with the direct detection method (Equation (1)), the ordinary heterodyne detection (Equation (3)) has the advantage of realizing the detection of the amplitude, frequency and phase of the signal light and improving the detection accuracy. It's good for detecting weak signals. According to the formula of photocurrent, it can be seen that the size of the photocurrent is proportional to the square root of the product of the power of the signal light and the local oscillator light. Therefore, when detecting weak signal, even if the signal light is very weak, as long as the local oscillator light power is large enough, a better signal can still be obtained eventually.

From Equation (5), it can be seen that balanced detection has advantages over single-source detection: on the one hand, it eliminates the DC component in the signal, which is convenient for signal processing, on the other hand, the amplitude of the AC component is double that of the output current of the single-source detector. In addition, due to the differential amplification used in the balanced detection, the common mode noise signals in the two detectors are greatly suppressed, and the signal-to-noise ratio of the output signals is improved. Dual balance detection not only has the advantage of balance detection, but also has a variety of modulation and demodulation methods, so its application prospect is very broad.

2.2. Link Noise Analysis

There are three types of noise in microwave photonic link: thermal noise, excess intensity noise and shot noise. The characteristics of each noise are analyzed in detail in the following sections [13].

Thermal noise is the noise caused by the Brownian motion of free electrons in the resistor. It has randomness and can only be increased but not eliminated. Therefore, in the balanced detection system, the thermal noise is the superposi-

tion of the thermal noise of the two detectors. If the resistance of the two detectors is equal, the thermal noise power is:

$$p_{th} = 4kT\Delta f. \tag{13}$$

where k is Boltzmann constant, T is the temperature, Δf is the bandwidth of the receiver.

Excess intensity noise is caused by fluctuations in local oscillator light output intensity and is usually described as relative intensity noise (RIN):

$$RIN = 10 \log \frac{\langle p_N^2 \rangle}{\langle p \rangle^2 \Delta f}. \tag{14}$$

where $\langle p_N^2 \rangle$ is the mean square value of noise power, $\langle p \rangle^2$ is the average output power of the laser, Δf is the bandwidth of the receiver. The unit of relative intensity noise is dBc/Hz. It can be seen that the mean square value of laser noise power is proportional to the relative intensity noise, and the value range of relative intensity noise is $-160 - -120$ dBc/Hz [14].

$$p_{rin} = 2e\gamma I_{dc}^2 \Delta f. \tag{15}$$

$$2e\gamma = 10^{\frac{RIN}{10}}. \tag{16}$$

where, γ represents the variation of noise power of the local oscillator with the square of the average power of the local oscillator. The unit is A^{-1} , and its corresponding value range is $10^2 - 10^6 A^{-1}$.

Assuming that the bandwidth of the two detectors is the same, since the excess intensity noise incident to the two detectors respectively is related, the square value of the excess intensity noise current of the balanced detector is [15]:

$$p_{rin} = 2e\gamma[\eta_1 \varepsilon E_1^2 - \eta_2(1-\varepsilon)E_1^2] \Delta f. \tag{17}$$

Shot noise is caused by the random fluctuation of photoelectric current in the photodetector. The shot noise current is a random process of Poisson distribution. The power spectral density of the shot noise is flat, so for the balanced detection system, the shot noise of the two signals after differential processing can be expressed as:

$$p_{sh} = 2eI_{DC} \Delta f = 2e(I_{DC1} + I_{DC2}) \Delta f. \tag{18}$$

Therefore, the SNR of the balanced detection method is:

$$\begin{aligned} SNR_{balance} &= \frac{i_{signal}^2}{p_{sh} + p_{rin} + p_{th}} \\ &= \frac{2e^2 E_S^2 E_L^2 (\eta_1 + \eta_2)^2 (1-\varepsilon) \varepsilon / h^2 \omega^2}{2 \frac{e^2}{h\omega} E_L^2 [\eta_1 \varepsilon + \eta_2(1-\varepsilon)] \Delta f + 2 \frac{e^3}{h^2 \omega^2} \gamma E_L^4 [\eta_1 \varepsilon - \eta_2(1-\varepsilon)]^2 \Delta f + 4kT \Delta f}. \end{aligned} \tag{19}$$

Compared with shot noise, thermal noise can often be ignored:

$$SNR_{balance} = \frac{(\eta_1 + \eta_2)^2 (1-\varepsilon) \varepsilon E_S^2 / h\omega}{(\eta_1 \varepsilon + \eta_2(1-\varepsilon)) \Delta f + \left(\frac{e}{h\omega}\right) \gamma E_L^2 [\eta_1 \varepsilon - \eta_2(1-\varepsilon)]^2 \Delta f}. \tag{20}$$

Assume that the photosensitive area of one of the balanced detectors is A_1 , and let A_1 approach to infinity or 0, then the signal-to-noise ratio formula of detector 1, namely ordinary heterodyne detection, is:

$$\begin{aligned} SNR_1 &= \frac{(A_1\eta_1 + \eta_2)^2 (1-\varepsilon)\varepsilon E_s^2 / h\omega}{(A_1\eta_1\varepsilon + \eta_2(1-\varepsilon))\Delta f + \left(\frac{e}{h\omega}\right)\gamma E_L^2 [A_1\eta_1\varepsilon - \eta_2(1-\varepsilon)]^2 \Delta f} \\ &= \frac{\eta_1(1-\varepsilon)E_s^2 / h\omega}{BW + \left(\frac{e}{h\omega}\right)\gamma E_L^2 \eta_1 \varepsilon \Delta f}. \end{aligned} \quad (21)$$

According to the SNR formula of Equation (20) for balanced coherent detection and the signal-to-noise ratio formula of Equation (21) for single source coherent detection, MATLAB software is used to carry out numerical simulation respectively. Some parameters in the SNR formula are as follows: the selected laser frequency is 150 THz, the photoelectric probe adopts InGaAs high-sensitivity PIN photoelectric diode, the band width $BW = 1.0 \times 10^6$ Hz, and the quantum efficiency is $\eta = 1$ A/W. It is assumed that the local oscillator power output by the fiber laser is 1 mW, and the signal light power is 0.1% of the local oscillator power, *i.e.*, 1 μ W. The relative intensity noise coefficient γ of the local oscillator light is 10^3 A⁻¹. Beam splitting ratio is variable, and the relation diagram of system noise and beam splitting ratio can be obtained.

It can be seen from **Figure 3(a)** that the maximum SNR of the balanced coherent detection system is 3.5 dB higher than that of the ordinary coherent detection. When the beam splitting ratio is 0.13 or 0.87, the SNR of the balanced coherent detection is exactly equal to that of the ordinary coherent detection. When the beam splitting ratio is less than 0.13 or more than 0.87, the SNR of the balanced coherent detection system is less than the SNR of the single source coherent detection.

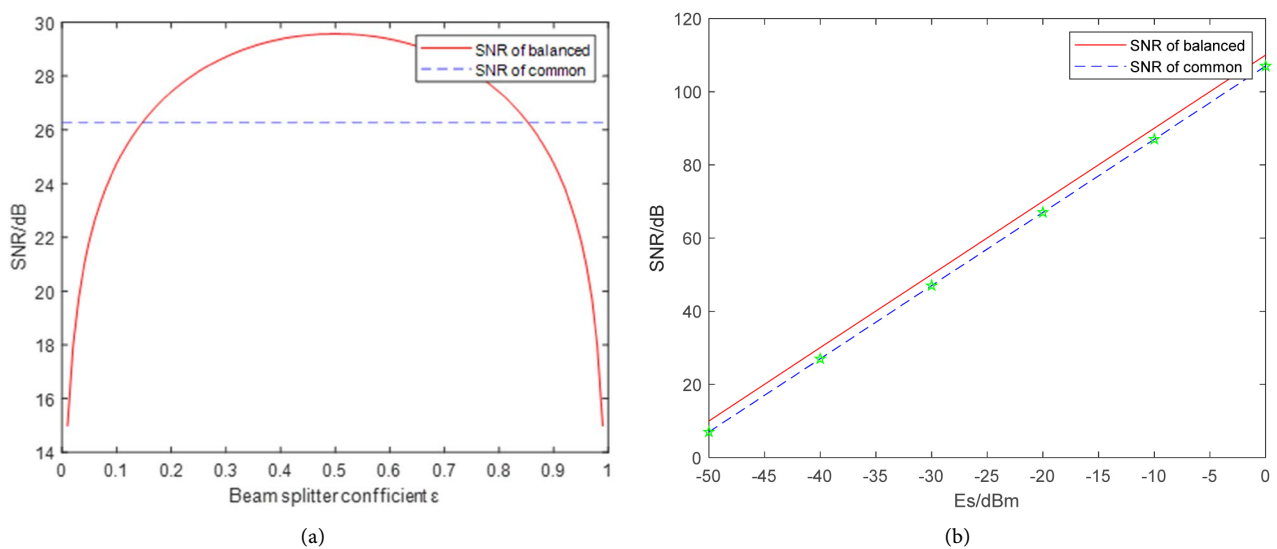


Figure 3. (a) Effect of beam splitting ratio on SNR; (b) Effect of signal optical power on SNR.

If the above conditions remain unchanged and the signal optical power is reduced from 0 dBm (1 mW) to -60 dBm (10^{-6} mW), the SNR of the balanced coherent detection system and the SNR of the single source coherent detection are shown in the **Figure 3(b)**.

It can be seen from the **Figure 3(b)** that the SNR of balanced detection is about 3 dB higher than that of ordinary heterodyne detection, under the condition that the signal optical power is taken as the variable.

3. Simulation and Discussion

3.1. Balance Detection System Simulation

The balance detection system model and the ordinary heterodyne detection system model are set as shown in **Figure 4(a)** and **Figure 4(b)**. The local oscillator light power is set as 1mW, and the signal light carrier frequency is 100 MHz. The polarization direction of the signal light is strictly the same as the local oscillator light. The photoelectric probe adopts PIN photoelectric diode with band width $BW = 1.0 \times 10^7$ Hz, and the value of quantum efficiency is $\eta = 1$ A/W. The signal light power is 0.1% of the local oscillator light power, that is, 1uW, and the relative intensity noise coefficient γ of the local oscillator light is 10^3 A⁻¹. THE beam splitting ratio is variable, and its simulation diagram is shown in **Figure 5(a)**.

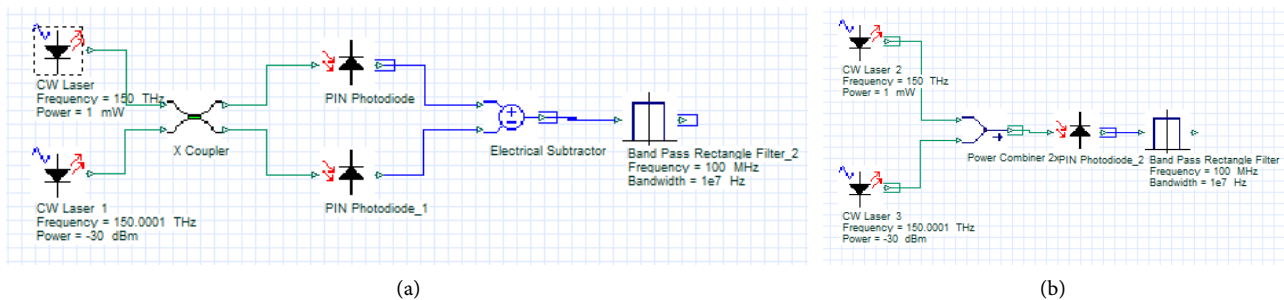


Figure 4. (a) Balance detection simulation diagram; (b) General heterodyne detection simulation diagram.

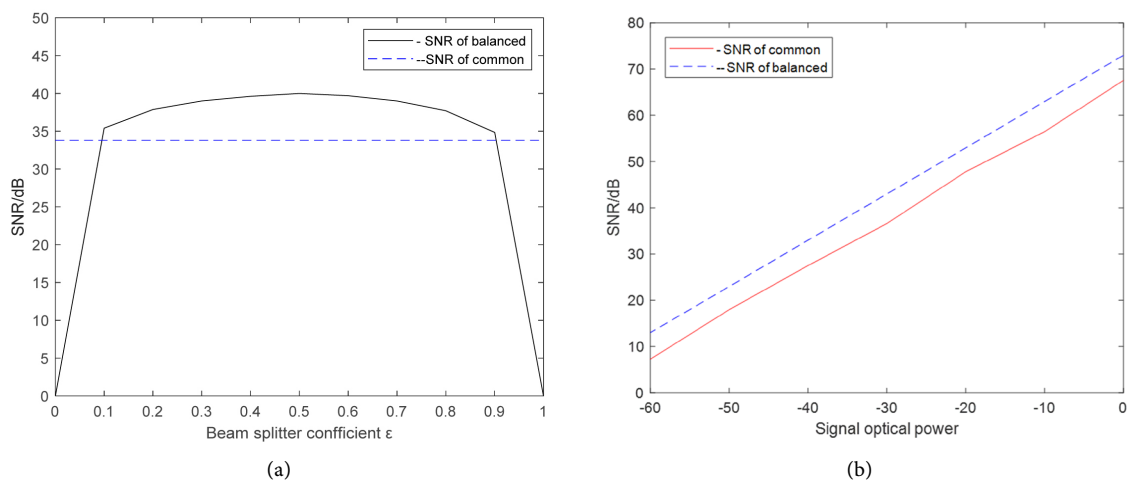


Figure 5. (a) The influence of beam splitting ratio on SNR; (b) Simulation diagram of the influence of signal optical power on SNR.

It can be seen from **Figure 5(a)** that the maximum SNR of the balanced coherent detection system is 5 dB higher than that of the ordinary coherent detection. When the beam splitting ratio is 0.10 or 0.90, the SNR of the balanced coherent detection is exactly equal to that of the ordinary coherent detection. When the beam splitting ratio is less than 0.10 or more than 0.90, the SNR of the balanced coherent detection system is less than the SNR of the single source coherent detection. The simulation results are basically consistent with the SNR formula derived by us, which verifies the correctness of the derivation.

As shown in **Figure 5(b)**, the SNR of balance detection is about 4 dB higher than that of ordinary heterodyne detection when the above conditions remain unchanged and the signal optical power is taken as variable, which is consistent with the theoretical results.

3.2. Simulation Analysis of Double Balance Detection System

The laser source is a continuous laser signal source, and the frequency is set to 150 THz. In order to make the difference frequency between the signal light and the local oscillator light exist, the frequency of the signal light is shifted by 1 G relative to the local oscillator light, that is, the difference frequency of the two signals is 1 G. The local oscillator light power is 10 mW, and the echo signal light power is 1 uW, both of which are linearly polarized light. Four PIN type photodetectors are selected, the response rate is 0.9 A/W, the dark current is 10 nA, and the noise characteristics of the detectors are the default of the system. The simulation diagram is shown in **Figure 6**.

Figure 7(a) and **Figure 7(b)** is the time domain simulation waveform diagram of the signals of system I and Q. It can be seen from the simulation results that the phase difference of the components of system I and Q is $\pi/2$.

Rotate the 1/4 wave plate and 1/2 wave plate respectively, and the simulation results are shown in **Figure 8** and **Figure 9**. When the 1/4 glass plate changes

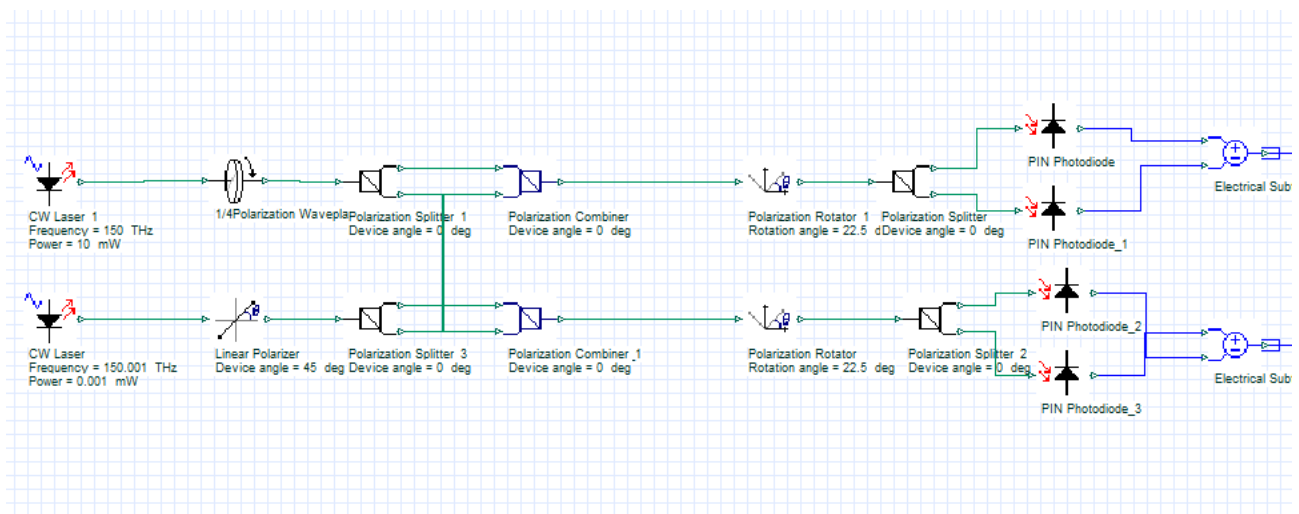


Figure 6. Simulation diagram of double balance detection.

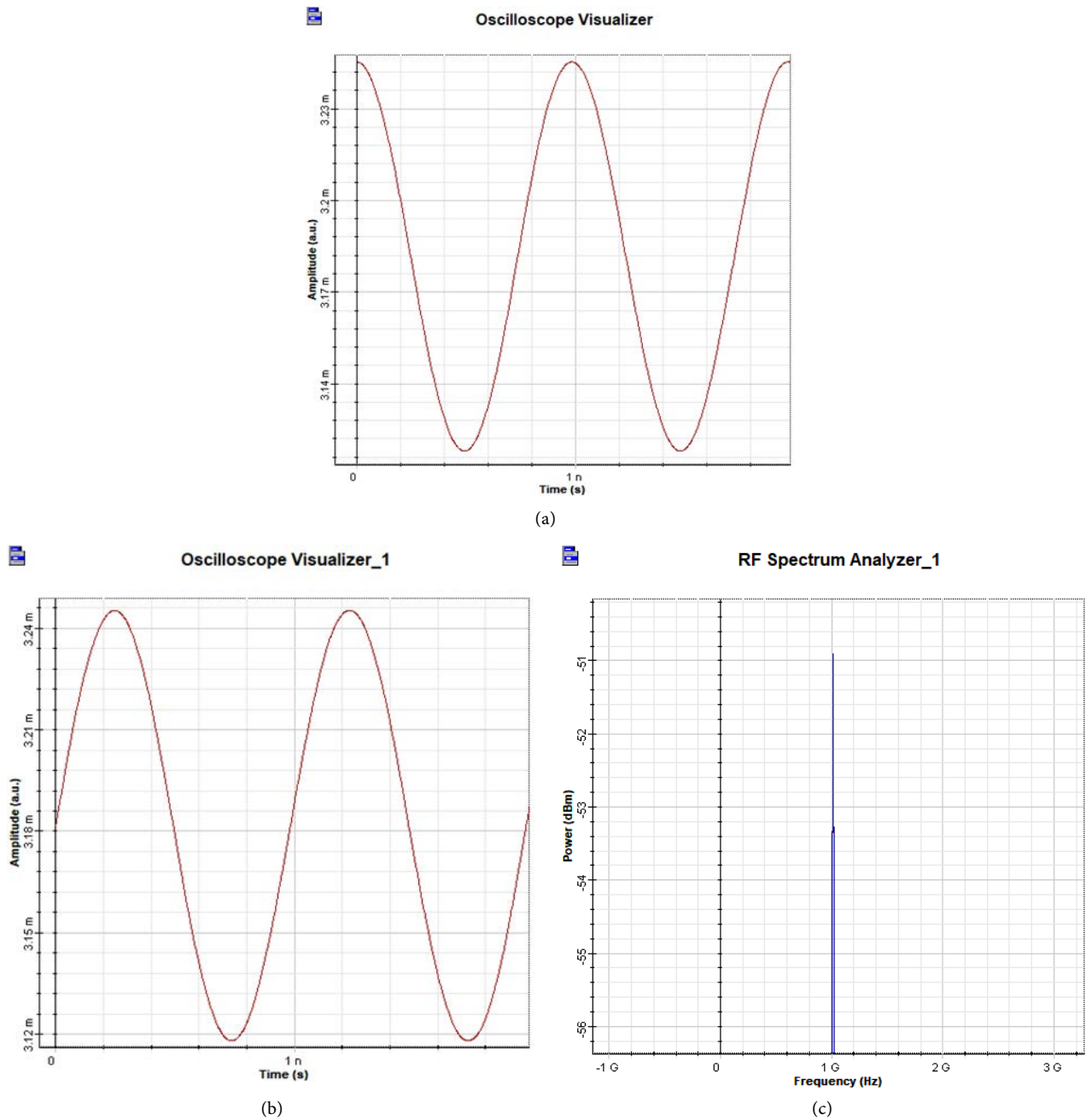


Figure 7. (a) is in-phase component (I) and (b) is quadrature component (Q), the simulation results that the phase difference of the components of system I and Q is $\pi/2$. (c) Difference frequency signal frequency domain waveform.

from a 45° polarization angle to a 20° polarization angle, the phase difference of signals in channel I and Q is not equal to $\pi/2$.

After the 1/2 glass slide was changed from 22.5° to 30° , the SNR is reduced by 3 dB.

Figure 7(c) is the frequency spectrum of the difference frequency signal. As can be seen from the figure, the difference frequency signal of 1 GHz can be demodulated after differential processing, and the detected signal also has a better power value.

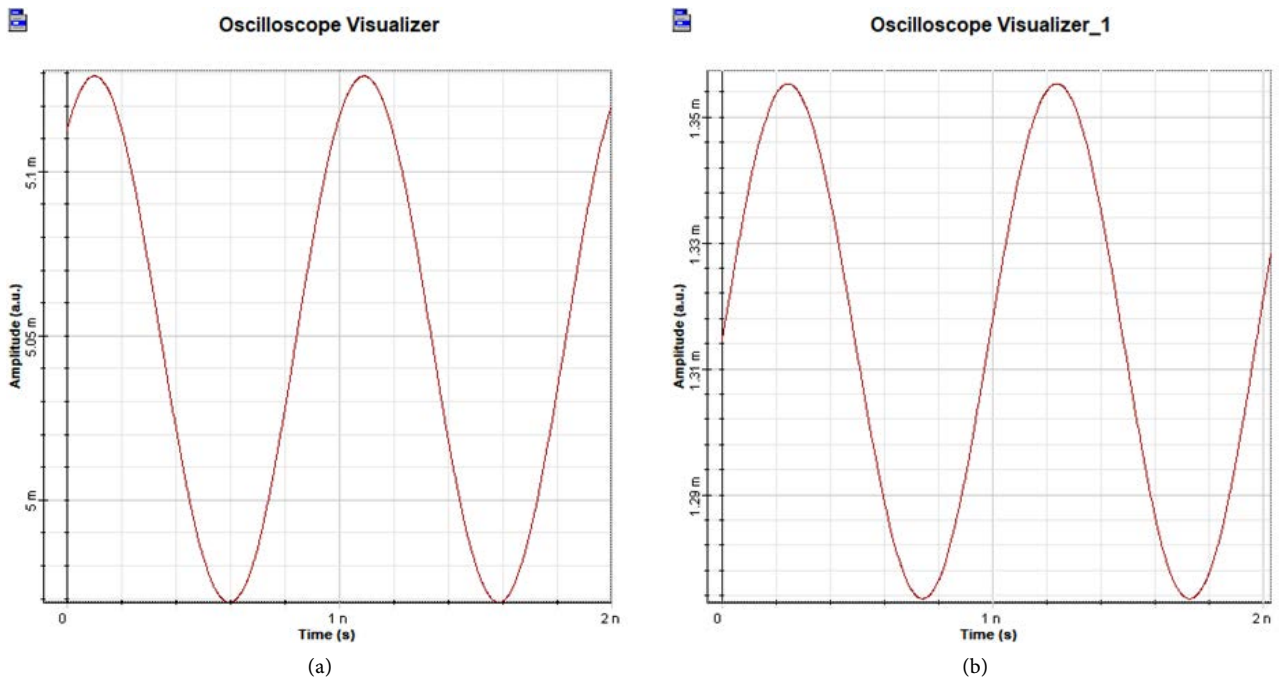


Figure 8. The 1/4 glass plate changes from a 45° polarization angle to a 20° polarization angle, the phase difference of signals in channel (a) and (b) is not equal to $\pi/2$ and the SNR was reduced by 2 dB.

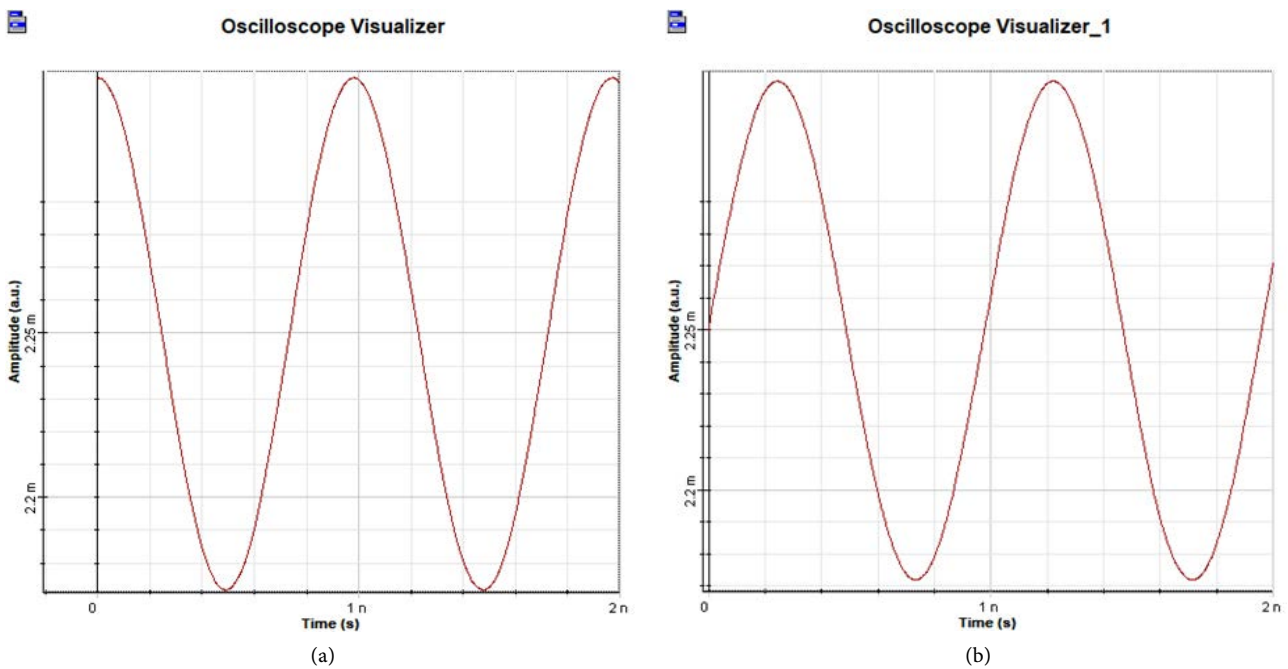


Figure 9. The 1/2 glass slide was changed from 22.5° to 30°, the SNR was reduced by 3 dB (from 41 dB To 38 dB).

4. Conclusion

This paper analyzes the working principle of the balanced heterodyne detection system, establishes the simulation models of ordinary heterodyne detection, balance detection and double balance detection system are built by OptiSystem. The simulation conclusion is consistent with the mathematical deduction. In the

double balanced detection simulation, from the different simulation results obtained from the rotation after the wave plate, we can draw the following conclusion. When 1/4 wave plate is 45° and the two 1/2 wave plates are at an angle of 22.5° with the incident light (corresponding to the splitting ratio similar to 0.5), the detected signal can obtain the Maximum power, the conclusion also studies double balanced heterodyne detection system of the best SNR conditions.

Funding

This work was supported by the National Natural Science Foundation of China under Grant 61875008.

Conflicts of Interest

The authors declare no conflicts of interest regarding the publication of this paper.

References

- [1] Svitek, R. and Raman, S. (2005) DC Offsets in Direct-Conversion Receivers: Characterization and Implications. *Microwave Magazine IEEE*, **6**, 76-86. <https://doi.org/10.1109/MMW.2005.1511916>
- [2] Eang, S.H., Choi, H.D., Yoon, S. and Cho, K. (2011) Application of Heterodyne Double Pass Interferometer on the Readout Sensor for a Biochemical Fluidic Channel. *IEEE*. <https://doi.org/10.1109/IQEC-CLEO.2011.6194124>
- [3] Onori, D., Laghezza, F., Scotti, F., Bartocci, M. and Ghelfi, P. (2016) A Direct-Conversion RF Scanning Receiver Based on Photonics. 2016 *IEEE/MTT-S International Microwave Symposium*, San Francisco, 22-27 May 2016. <https://doi.org/10.1109/MWSYM.2016.7540327>
- [4] Zhu, X., Jin, T., Chi, H., Tong, G. and Lai, T. (2018) A Coherent Photonic RF Scanning Receiver Based on a Flat Optical Frequency Comb. *Optics Communications*, **421**, 41-45. <https://doi.org/10.1016/j.optcom.2018.03.054>
- [5] Jing, L., Xiao, W., Zhu, X. and Zhang, C., *et al.* (2010) A High Sensitivity and Wide Dynamic Range Zero-If RF Receiver for Cognitive Radio Application. *Journal of Electronics*, **27**, 696-700. <https://doi.org/10.1007/s11767-011-0499-7>
- [6] Chan, V.W.S. (2006) Free-Space Optical Communications. *Journal of Lightwave Technology*, **24**, 4750-4762. <https://doi.org/10.1109/JLT.2006.885252>
- [7] Seimetz, M. and Weinert, C.M. (2006) Options, Feasibility, and Availability of 2 × 4 90° Hybrids for Coherent Optical Systems. *Journal of Lightwave Technology*, **24**, 1317-1322. <https://doi.org/10.1109/JLT.2005.863251>
- [8] Savory, S.J. (2010) Digital Coherent Optical Receivers: Algorithms and Subsystems. *IEEE Journal of Selected Topics in Quantum Electronics*, **16**, 1164-1179. <https://doi.org/10.1109/JSTQE.2010.2044751>
- [9] Seimetz, M. (2009) High-Order Modulation for Optical Fiber Transmission. Springer Berlin Heidelberg. <https://doi.org/10.1007/978-3-540-93771-5>
- [10] Lygagnon, D.S., Katoh, K. and Kikuchi, K. (2005) Unrepeated 210-km Transmission with Coherent Detection and Digital Signal Processing of 20-Gb/s QPSK Signal. <https://doi.org/10.1007/978-3-540-93771-5>
- [11] Yu, J., Singh, U.N., Barnes, J.C., Barnes, N.P. and Petros, M. (2001) High-Energy

-
- 2- μm Laser for Multiple Lidar Applications. *Proceedings of SPIE—The International Society for Optical Engineering*, **4153**, 70-77. <https://doi.org/10.1117/12.417025>
- [12] Frehlich, R., Hannon, S.M. and Henderson, S.W. (1994) Performance of a 2-m Coherent Doppler Lidar for Wind Measurements. *J. Atmos. Oceanic Technol.*, **11**, 1517-1528. [https://doi.org/10.1175/1520-0426\(1994\)011<1517:POACDL>2.0.CO;2](https://doi.org/10.1175/1520-0426(1994)011<1517:POACDL>2.0.CO;2)
- [13] Wang, C., Amzajerdian, F. and Gao, C.Q. (2009) Investigation of Balanced Detection and Receiver for Coherent Lidar. *Proceedings of SPIE—The International Society for Optical Engineering*, **7382**, 73820I. <https://doi.org/10.1117/12.829459>
- [14] Chen, B., Fan, Y. and Gao, Y. (2020) Wideband Coherent Optical RF Channelizer with Image-Reject Down-Conversion. *Asia Communications and Photonics Conference*. <https://doi.org/10.1364/ACPC.2020.M4A.335>
- [15] Park, Y. and Cho, K. (2011) Heterodyne Interferometer Scheme Using a Double Pass in an Acousto-Optic Modulator. *Optics Letters*, **36**, 331-333. <https://doi.org/10.1364/OL.36.000331>